

ORIGINAL RESEARCH

## Composite biomarkers defined by multiparametric immunofluorescence analysis identify ALK-positive adenocarcinoma as a potential target for immunotherapy

Hélène Roussel<sup>a,b,c,\*</sup>, Eléonore De Guillebon<sup>a,c,d,\*</sup>, Lucie Biard<sup>e</sup>, Marion Mandavit<sup>a,c</sup>, Laure Gibault<sup>b</sup>, Elisabeth Fabre<sup>d</sup>, Martine Antoine<sup>f,g</sup>, Paul Hofman<sup>h</sup>, Michèle Beau-Faller<sup>i</sup>, Hélène Blons<sup>j</sup>, Claire Danel<sup>k</sup>, Françoise Le Pimpec Barthes<sup>l</sup>, Alain Gey<sup>a,m</sup>, Clémence Granier<sup>a,c,m</sup>, Marie Wislez<sup>g,n</sup>, Pierre Laurent-Puig<sup>j</sup>, Stéphane Oudard<sup>a,c,d</sup>, Patrick Bruneval<sup>b</sup>, Cécile Badoual<sup>a,b,c</sup>, Jacques Cadranet<sup>g,n</sup>, and Eric Tartour<sup>a,c,m</sup>

<sup>a</sup>INSERM U970, Université Paris Descartes, Sorbonne Paris Cité, Paris, France; <sup>b</sup>Department of Pathology, Hôpital Européen Georges Pompidou, Paris, France; <sup>c</sup>Equipe Labellisée Ligue Contre le Cancer, Paris, France; <sup>d</sup>Department of Oncology, Hôpital Européen Georges Pompidou, Paris, France; <sup>e</sup>Department of Biostatistics and Medical Information, Hôpital Saint Louis, Paris, France; <sup>f</sup>Department of Pathology, Hôpital Tenon, Paris, France; <sup>g</sup>GRC04 Théranscan, Université P&M Curie, Paris, France; <sup>h</sup>Department of Pathology, Hôpital Pasteur, Nice, France; <sup>i</sup>Department of Biochemistry and Molecular Biology, Hôpital de Hautepierre Strasbourg, Strasbourg, France; <sup>j</sup>Department of Biochemistry and Molecular Biology INSERM UMR-S 1147, Hôpital Européen Georges Pompidou, Paris, France; <sup>k</sup>Department of Pathology Pompidou, Hôpital Bichat, Paris, France; <sup>l</sup>Department of Thoracic Surgery, Hôpital Européen Georges Pompidou, Paris, France; <sup>m</sup>Service d'Immunologie biologique, Hôpital Européen Georges Pompidou, APHP, Paris, France; <sup>n</sup>Department of Pneumology, Hôpital Tenon, APHP, Paris, France

### ABSTRACT

Anaplastic lymphoma kinase (ALK) inhibitors have been successfully developed for non-small cell lung carcinoma (NSCLC) displaying chromosomal rearrangements of the *ALK* gene, but unfortunately resistance invariably occurs. Blockade of the PD-1/PD-L1/2 inhibitory pathway constitutes a breakthrough for the treatment of NSCLC. Some predictive biomarkers of clinical response to this therapy are starting to emerge, such as PD-L1 expression by tumor/stromal cells and infiltration by CD8<sup>+</sup> T cells expressing PD-1. To more effectively integrate all of these potential biomarkers of clinical response to immunotherapy, we have developed a multiparametric immunofluorescence technique with automated immune cell counting to comprehensively analyze the tumor microenvironment of ALK-positive adenocarcinoma (ADC). When analyzed as either a continuous or a dichotomous variable, the mean number of tumor cells expressing PD-L1 ( $p = 0.012$ ) and the percentage of tumor cells expressing PD-L1 were higher in ALK-positive ADC than in *EGFR*-mutated ADC or WT (non-*EGFR*-mutated and non-*KRAS*-mutated) NSCLC. A very strong correlation between PD-L1 expression on tumor cells and intratumoral infiltration by CD8<sup>+</sup> T cells was observed, suggesting that an adaptive mechanism may partly regulate this expression. A higher frequency of tumors combining positive PD-L1 expression and infiltration by intratumoral CD8<sup>+</sup> T cells or PD-1<sup>+</sup>CD8<sup>+</sup> T cells was also observed in ALK-positive lung cancer patients compared with *EGFR*-mutated ( $p = 0.03$ ) or WT patients ( $p = 0.012$ ). These results strongly suggest that a subgroup of ALK-positive lung cancer patients may constitute good candidates for anti-PD-1/PD-L1 therapies.

### ARTICLE HISTORY

Received 13 December 2016  
Accepted 20 January 2017

### KEYWORDS

ALK-positive adenocarcinoma; immunotherapy; *in situ* quantitative cell imaging; predictive biomarker; tumor microenvironment

## Introduction

Anaplastic lymphoma kinase (*ALK*) rearrangement with *nucleo-plasmin* (*NPM*), first identified in anaplastic large cell lymphoma, has been found in other tumors with certain differences in terms of the selected fusion partner.<sup>1,2</sup> Approximately 5% to 6% of non-small cell lung carcinomas (NSCLC) present chromosomal rearrangements of the *ALK* gene, mainly involving the *echinoderm microtubule-associated protein-like 4* (*EML4*) gene as partner.<sup>3</sup> In all of these chimeric proteins, ALK is constitutively activated and considered to be a driver for tumor cell proliferation and survival.<sup>4</sup>

The ALK tyrosine kinase inhibitor (TKI), crizotinib, has been successfully developed in these patients with a high initial clinical response rate. Unfortunately, resistance invariably occurs leading to tumor relapse and eventually to the patient's

death.<sup>5</sup> Despite the development of novel ALK TKIs, such as ceritinib and alectinib, which partially overcome crizotinib resistance, other therapeutic approaches should be proposed in combination with TKIs for these patients.

Reversal of immunosuppression in the tumor microenvironment via targeting of inhibitory receptors expressed by T cells (Programmed cell Death protein 1 (PD-1), Cytotoxic T lymphocyte-associated antigen 4 (CTLA-4) or their ligands (Programmed Death Ligand 1 (PD-L1) constitutes a major breakthrough in the treatment of cancer. In patients with locally advanced or metastatic NSCLC who have received at least one prior line of chemotherapy or TKIs, two anti-PD-1 antibodies, nivolumab (Opdivo<sup>®</sup>) and pembrolizumab (Keytruda<sup>®</sup>) were recently approved by the US Food Drug Administration and European Medicines Agency.<sup>6-8</sup> In the

pembrolizumab recommended indication, the tumor has to express PD-L1. Since the overall response rate to blockade of the PD-1/PD-L1 pathway in NSCLC ranges between 25 and 30%, predictive biomarkers of clinical response need to be identified. The current dogma states that these immunotherapeutic agents unleash the cytotoxic activity of antitumor CD8<sup>+</sup> T cells already present in the tumor microenvironment, but maintained in an anergic state by the interaction between PD-1 and their ligands (PD-L1 and PD-L2). This natural immune response is dictated by the immunogenicity of the tumor based on its ability to generate neoepitopes secondary to mutations or gene rearrangements, more easily recognized by CD8<sup>+</sup> T cells.<sup>9</sup> The presence of virus or pathogens in the tumor and, in some cases, the likely recognition of self-antigens shared by normal and tumor cells, may also trigger priming of an antitumor immune response that would also explain the autoimmune side effects of immunotherapy. As expected, a high non-synonymous mutational tumor burden resulting in class I neoantigen load detected by an *in silico* algorithm may predict clinical benefit in NSCLC patients,<sup>10</sup> and in other cancer patients treated by anti-PD-1/PD-L1.<sup>11-13</sup> However, low mutational load did not preclude clinical response to immunotherapy.<sup>14,15</sup> PD-L1 expression by tumor and/or immune cells has also been associated with improved clinical benefit to PD-1 pathway blockade in NSCLC patients.<sup>7,8,16,17</sup> However, baseline PD-L1 expression did not appear to predict clinical response in patients with squamous cell carcinoma of the lung.<sup>6,8</sup> The clinical predictive value of PD-L1 may vary depending on the clinical outcome selected (overall response rate, progression-free survival, overall survival (OS)), the criteria used to determine the positivity of PD-L1 staining (cut-off, tumor versus stroma), and the type of tumor analyzed.<sup>14,18</sup> Furthermore, the pre-existence of CD8-positive tumor-infiltrating lymphocytes, whether or not they express PD-1, has been correlated with the benefit of anti-PD-1 therapy in melanoma,<sup>19</sup> MicroSatellite Instability (MSI)-high colorectal carcinomas<sup>11</sup> and urothelial tumors,<sup>12</sup> but this association has not been confirmed by other groups in melanoma<sup>20,21</sup> or in other tumors.<sup>22,23</sup> Activated CD8<sup>+</sup> T cells identified by their PD-L1 expression or the detection of PD-1 by immune cells have also been correlated with clinical response to anti-PD-1.<sup>19,22</sup> In the light of these results, composite biomarkers integrating various components of host-tumor interaction combined in a “tumor-immune signature” may be more relevant to guide the selection of potential responding patients to immunotherapy. In line with this hypothesis, classification of tumors based on their levels of PD-L1 expression and CD8<sup>+</sup> T cell infiltration has been proposed.<sup>24,25</sup>

The ALK-rearranged protein is immunogenic in cancer patients, as lymphoma patients with ALK rearrangements mount spontaneous B- and T-cell responses against the ALK protein.<sup>26,27</sup> Various ALK chimeric proteins expressed in anaplastic lymphoma and NSCLC patients have been shown to induce PD-L1.<sup>28,29</sup> Few studies have analyzed intratumoral T cell infiltration in tumors with ALK rearrangement. In a small number of ALK-positive patients (n = 5), Voena et al. reported a low percentage of infiltrating T cells, while in ALK-driven lung cancer in mice, an accumulation of PD-1<sup>+</sup> T cells was reported compared with lung tumors without ALK rearrangement.<sup>30</sup> To more effectively integrate all of

these potential biomarkers of clinical response to immunotherapy, we have developed an immunofluorescence platform to comprehensively analyze the tumor microenvironment of ALK-positive adenocarcinoma (ADC). We compared our results with a series of patients harboring epidermal growth factor receptor (EGFR) mutations or patients without the major dominant mutations found in NSCLC (EGFR and K-RAS). Based on analysis of their tumor microenvironment, we found that a subpopulation of ALK-positive ADC displays various criteria associated with clinical response to PD-1/PD-L1 blockade.

## Results

### Comparative analysis of immune cell infiltration in ALK-positive, EGFR-mutated ADC and WT tumors

Based on CK19 staining of tumor cells, tissues were segmented between intratumoral and stromal zones to precisely locate immune cell infiltration (Fig. 1). Various types of triple immunofluorescence staining (CK19-CD8-PD-1, CK19-CD4-Foxp3) were developed to quantitate intratumoral or stromal infiltration of CD8<sup>+</sup> T cells, PD-1<sup>+</sup>CD8<sup>+</sup> T cells, CD4<sup>+</sup> T cells and Foxp3<sup>+</sup>CD4<sup>+</sup> regulatory T cells (Fig. 1 and Fig. S1). The mean total number of CD8<sup>+</sup> T cells expressing PD-1 was not significantly different between the various subgroups of lung cancer (Figs. 2A and B). In contrast, EGFR-mutated ADC were less intensely infiltrated by intratumoral CD8<sup>+</sup> T cells and intratumoral PD-1<sup>+</sup>CD8<sup>+</sup> T cells than WT tumors (Fig. 2C and D). The number of intratumoral PD-1<sup>+</sup>CD8<sup>+</sup> T cells tended to be higher in the ALK-positive ADC group compared with the EGFR-mutated group (*p* = 0.06) (Fig. 2D).

Most total and intratumoral CD8<sup>+</sup> T cells expressed PD-1. For example, 93% of intratumoral CD8<sup>+</sup> T cells expressed PD-1 in the ALK-positive ADC group versus 78% in the EGFR-mutated group and 81% in the WT group with no significant difference between the various groups.

Since, the antitumor activity of CD8<sup>+</sup> T cells requires the expression of MHC class I molecules by tumor cells, we also checked for MHC class I expression using an H score (Fig. S2). No significant differences in  $\beta$ 2-microglobulin expression – the invariable chain of HLA class I molecules – were observed between the various subgroups of lung cancer patients (Fig. S2). The mean total number of CD4<sup>+</sup> T cells infiltrating all lung cancer subgroups was more than tenfold higher than the total number of CD8<sup>+</sup> T cells (Fig. S1B and Fig. 2). In all subgroups, CD4<sup>+</sup> T cells and regulatory T cells were mainly found in the stroma (Fig. S1A and data not shown). No significant differences in infiltration by the various subpopulations of CD4<sup>+</sup> T cells or in the CD8<sup>+</sup>/regulatory T cell ratio were observed between the various subgroups of lung cancer patients (Figs. S1B and D).

### PD-L1 expression in ALK-positive, EGFR-mutated and WT lung cancer

To accurately discriminate PD-L1 expression by tumor cells and stromal/immune cells, we performed double immunofluorescence staining for PD-L1 combined with CK19

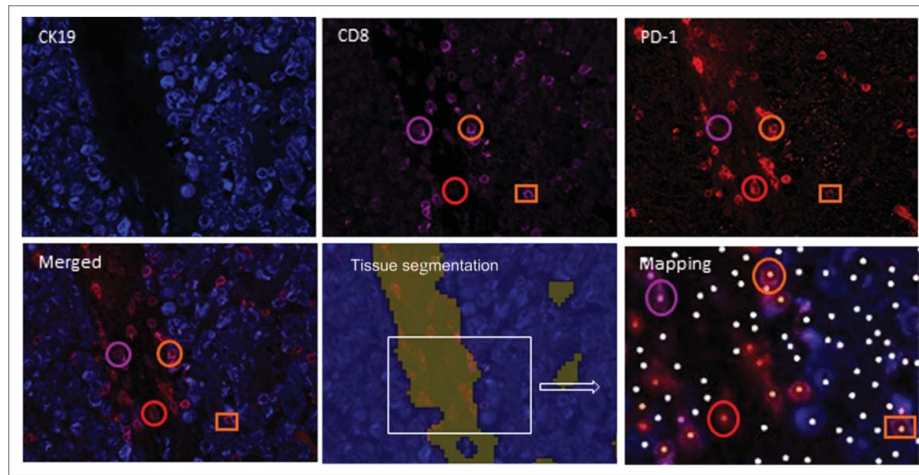


**Figure 1.** Infiltration of PD-1<sup>+</sup>CD8<sup>+</sup> T cells and CD8<sup>+</sup> T cells in the tumor nest and stroma of a lung cancer patient. Frozen tissue sections were stained with antibodies to detect PD-1, CD8 and CK19. Using InForm<sup>®</sup> software, tissue segmentation was performed on the basis of CK19 staining to determine tumor nest (blue) and stromal areas (other color). Circles identify cells in the stroma and squares identify the presence of cells in the tumor nest. A phenotyping procedure based on “training” of the software to recognize positive and negative cells was performed. Mapping determined the phenotype of the cells (PD-1<sup>+</sup>CD8<sup>+</sup>: orange dot; PD-1<sup>-</sup>CD8<sup>+</sup>: pink dot, PD-1<sup>+</sup>CD8<sup>-</sup>: red dot, other cells: white dot) and allowed automated counting. For example, orange circles identify PD-1<sup>+</sup>CD8<sup>+</sup> stromal cells, while pink circles identify PD-1<sup>-</sup>CD8<sup>+</sup> cells in the stroma (pink dot on mapping) (original magnification  $\times 200$ ).

(Fig. 3). In ALK-positive ADC, the median number of tumor cells expressing PD-L1 per field was 13.6 (IQR: 1.2–103)(Fig. 4A). Using various cut-offs for the percentage of tumor cells expressing PD-L1 per field to define tumor PD-

L1 expression as a dichotomous variable, we found that 62% (Fig. 4D), 45% (Fig. 4E) and 17% (Fig. 4F) of patients expressed PD-L1 using cut-offs of 1%, 10% and 50%, respectively. Expressed as either a continuous or a

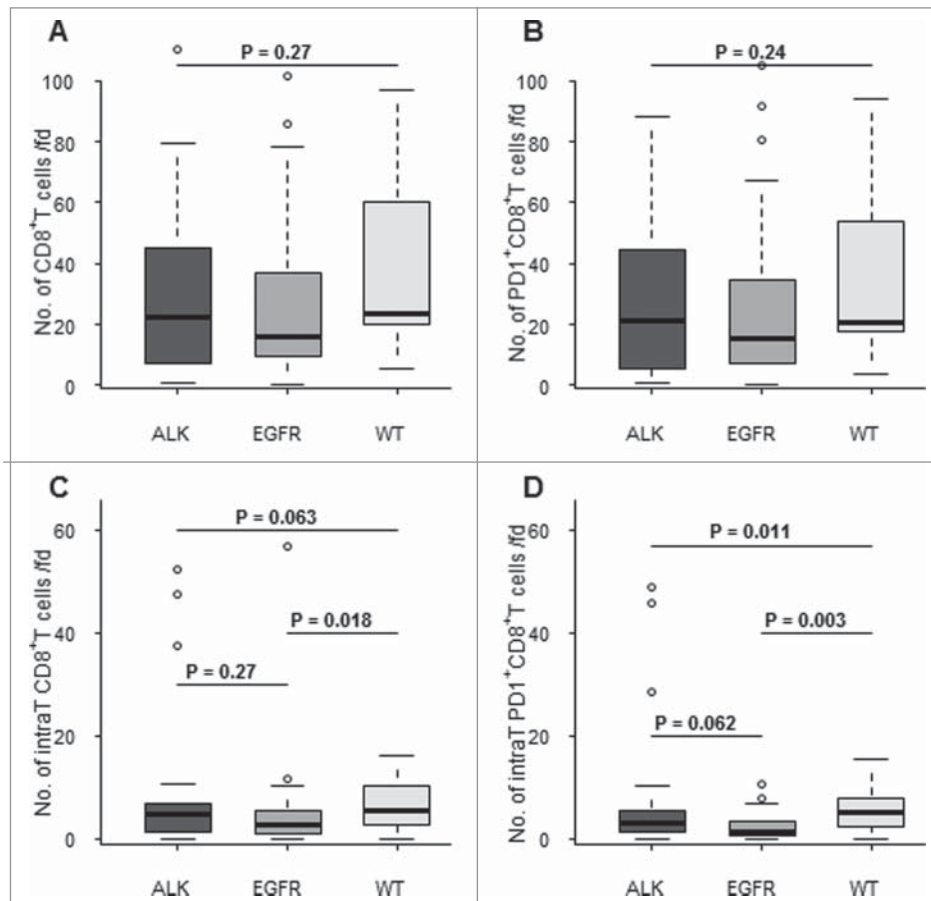


**Figure 2.** Comparative analysis of PD-1<sup>+</sup>CD8<sup>+</sup> T cell and CD8<sup>+</sup> T cell infiltration between various molecular subgroups of lung cancer patients. The number of total (A, B) and intratumoral (C,D) PD-1<sup>+</sup>CD8<sup>+</sup> T cells (B,D) and total CD8<sup>+</sup> T cells (A,C) was quantitated per field (fd) by a multiparametric immunofluorescence technique between three lung cancer subgroups (ALK = ALK-positive cancer, EGFR = EGFR-mutated, and WT = non-ALK-positive, non-EGFR-mutated and non-KRAS-mutated lung cancer). Mean numbers of cells were compared between subgroups using Kruskal–Wallis (three subgroups) or Wilcoxon’s rank sum (two subgroups) test. \* $p < 0.05$ .



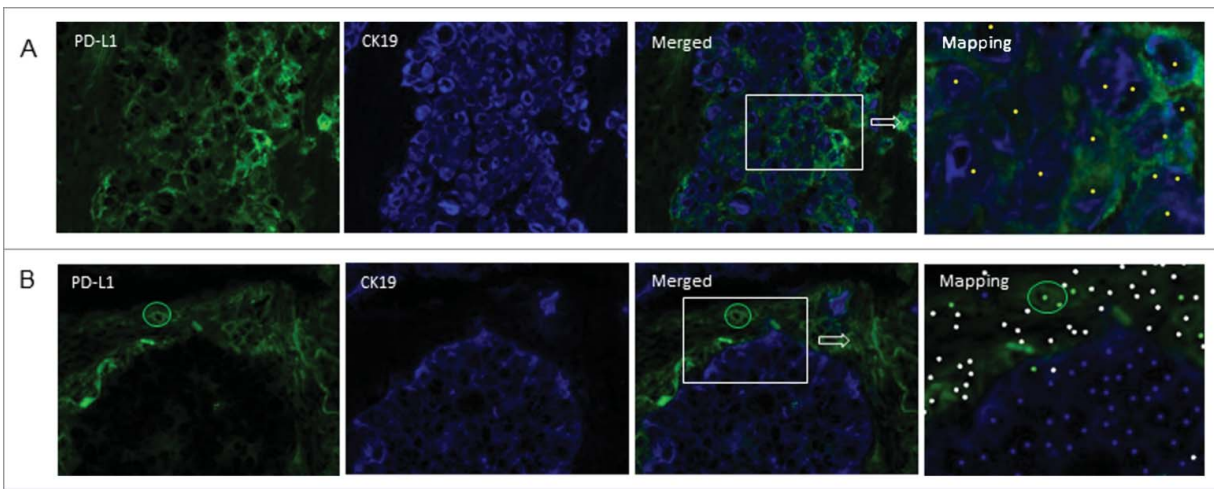


**Figure 3.** PD-L1 expression on tumor and or stromal/immune cells. Frozen tissue sections derived from patients with lung adenocarcinoma were double-stained by immunofluorescence (CK19 (blue), PD-L1 (green)). Tissue segmentation was performed on the basis of CK19 staining to determine tumor nest and stromal areas. A phenotyping step based on “training” of the software to recognize positive and negative cells was then performed generating an analysis algorithm. Mapping determined the phenotype of the cells (CK19<sup>+</sup>PD-L1<sup>-</sup>: blue dot; CK19<sup>+</sup>PD-L1<sup>+</sup>: yellow dot; CK19<sup>-</sup>PD-L1<sup>+</sup>: green dot; other cells: white dot). Positive (A) and negative (B) staining of tumor cells for PD-L1 is shown. The circle in B identifies PD-L1-positive cells in the stroma (original magnification  $\times 200$ ).

dichotomous variable, the mean number of tumor cells expressing PD-L1 ( $p = 0.012$ ) (Fig. 4A) and the percentage of tumor cells expressing PD-L1 (Figs. 4D–F) were higher in ALK-positive ADC than in EGFR-mutated ADC or WT lung cancer, regardless of the cut-off used (Figs. 4D–F). For example, 45% of ALK-positive ADC expressed PD-L1 on tumor cells with a cut-off of 10%, while this percentage decreased to 26% for EGFR-mutated ADC and 8% for WT lung cancers (Fig. 4E). In ALK-positive ADC, the number of stromal/immune cells expressing PD-L1 (median 5.2; IQR (1.6–11.6)) was lower than the number of tumor cells

expressing PD-L1 (median 13.6,  $p = 0.011$ ) (Figs. 4A and B). This predominance of PD-L1-expressing tumor cells over stromal/immune cells was not observed in EGFR-mutated and WT tumors (Figs. 4A and B). The number of non-epithelial stromal/immune cells expressing PD-L1 was not significantly different between the various subgroups of patients (Fig. 4B), while the total number of PD-L1-expressing cells (both tumor cells and stromal/immune cells) was also higher in ALK-positive ADC than in the other lung cancer subgroups ( $p = 0.002$ ) (Fig. 4C). Very few CD8<sup>+</sup> T cells expressed PD-L1 (data not shown).

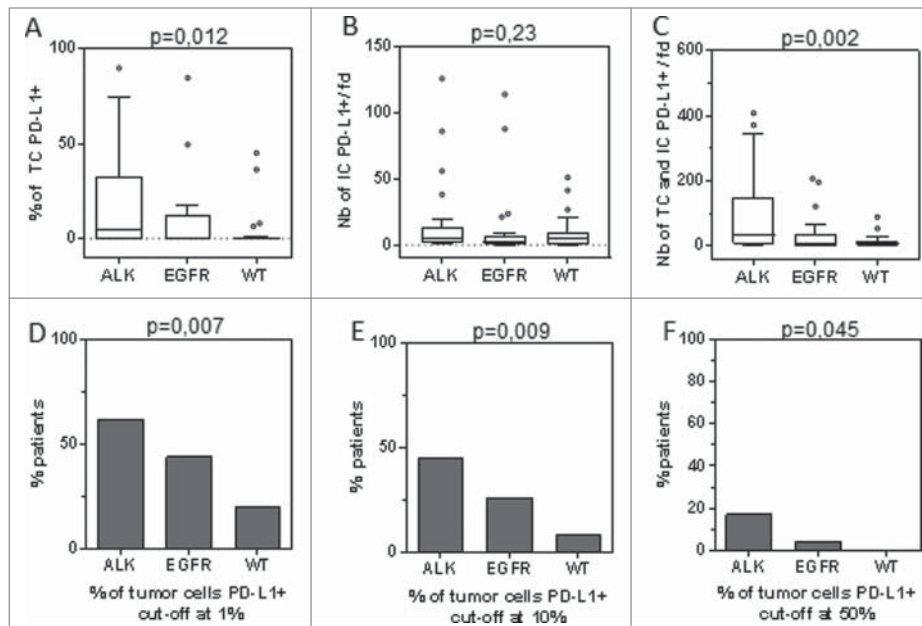


**Figure 4.** Comparative analysis of PD-L1 expression on tumor cells (TC) and immune cells (IC) with various molecular subgroups of lung cancer patients (ALK-positive, EGFR-mutated and WT (non-EGFR-mutated, non-KRAS-mutated, non-ALK-positive)). PD-L1 was quantitated as a continuous variable and either as a percentage of tumor cells (A), number of PD-L1<sup>+</sup> stromal/immune cells per field (fd)(B), or total number of PD-L1<sup>+</sup> tumor cells and PD-L1<sup>+</sup> stromal cells per field (C). These parameters were compared between the three subgroups of lung cancer patients. Percentage of patients whose tumors expressed PD-L1 with cut-offs greater than 1% (D), 10% (E) and 50% (F).

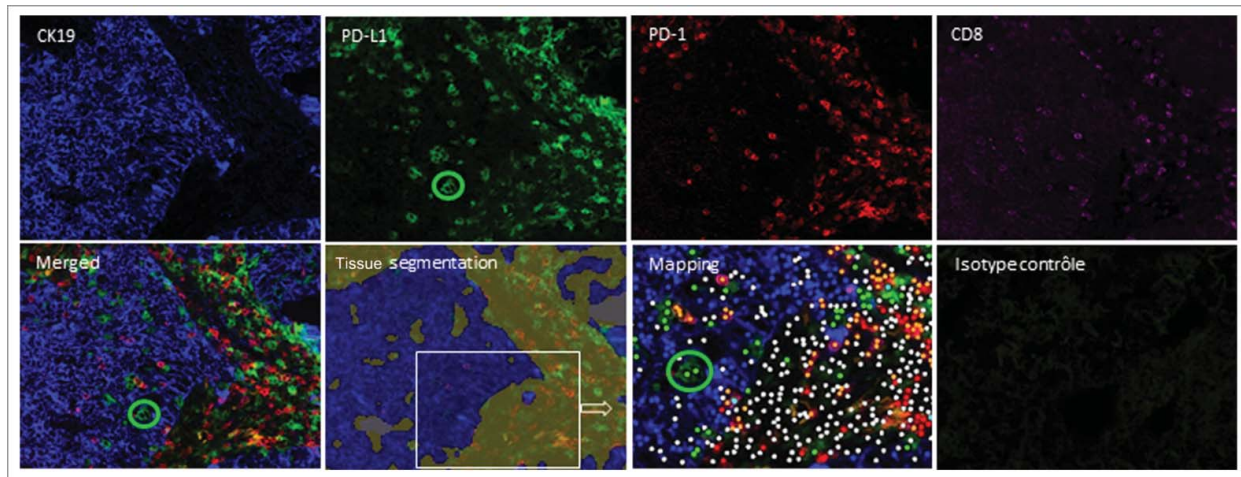


**Figure 5.** Difficulties in the interpretation of PD-L1 staining in the tumor nest. Frozen tissue sections derived from patients with lung adenocarcinoma were quadruplex stained by immunofluorescence (CK19 (blue), PD-L1 (green), PD-1 (red) and CD8 (pink)) on the same slide. Tissue segmentation was performed on the basis of CK19 staining to determine tumor and stromal areas. Mapping determined the phenotype of the cells with the corresponding code: CK19<sup>+</sup>PD-L1<sup>-</sup>: blue dot; CK19<sup>+</sup>PD-L1<sup>+</sup>: yellow dot; CK19<sup>-</sup>PD-L1<sup>+</sup>: green dot; PD-1<sup>+</sup>CD8<sup>+</sup>: orange dot; PD-1<sup>-</sup>CD8<sup>+</sup>: pink dot; PD-1<sup>+</sup>CD8<sup>-</sup>: red dot, other cells: white dot). The green circle identifies PD-L1<sup>+</sup>CK19<sup>-</sup> cells infiltrating the tumor nest (original magnification  $\times 200$ ).

No significant correlation was observed between PD-L1 expression on tumor cells and stromal/immune cells (data not shown).

In the literature, PD-L1 expression is usually assigned to tumor cells or stromal cells according to the region in which the staining is observed. Using quadruple immunostaining (CK19, PD-L1, CD8, PD-1), we clearly demonstrated that, in some patients, PD-L1-positive cells in the tumor nest did not correspond to either tumor cells in the absence of CK19 co-staining or CD8<sup>+</sup> T cells (Fig. 5). Only this type of multiparametric technique is able to discriminate these cells from PD-L1-positive tumor cells. This study therefore highlights a possible bias in quantitation of PD-L1 on tumor cells using conventional immunohistochemistry techniques.

### Correlation between immune cell infiltration and tumor phenotype (PD-L1 and MHC class I)

A significant correlation was demonstrated between the number of total or intratumoral CD8<sup>+</sup> T cells (Figs. 6A and B) or PD-1<sup>+</sup>CD8<sup>+</sup> T cells (Figs. 6C and D) and PD-L1 expression by tumor cells, suggesting a possible role of adaptive immunity in the regulation of PD-L1 on tumor cells in *ALK*-positive ADC. Interestingly, no correlation was observed between PD-L1 expression by tumor cells and total or intratumoral PD-1<sup>+</sup>CD8<sup>+</sup> T and CD8<sup>+</sup> T cell infiltration in *EGFR*-mutated ADC (Fig. S3). In addition, using quadruple immunostaining for CK19, PD-L1, PD-1 and CD8<sup>+</sup>, we clearly demonstrated close contact between PD-L1<sup>+</sup> tumor cells and PD-1<sup>+</sup>CD8<sup>+</sup> T cells in some *ALK*-positive ADC (Fig. S4).

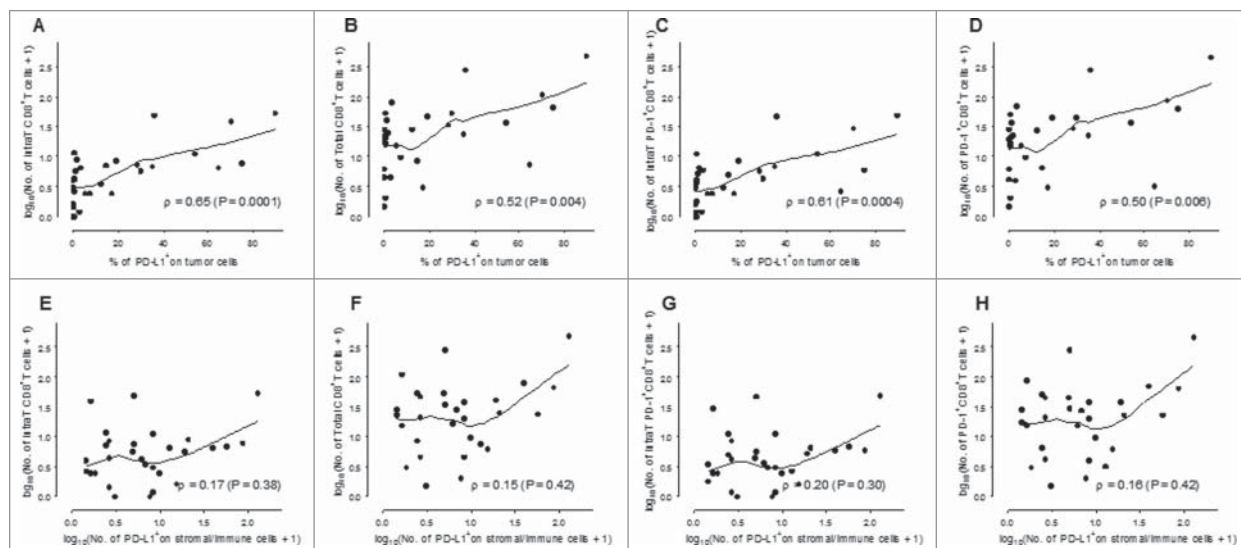


**Figure 6.** Correlation between the number of infiltrating CD8<sup>+</sup> T cells and the percentage of PD-L1 expression on tumor cells. In *ALK*-positive lung cancer patients, the percentage of PD-L1 expression on tumor cells (A–D) and the mean number of PD-L1<sup>+</sup> stromal/immune cells (E–H) was plotted against the number of intratumoral (intraT) CD8<sup>+</sup> T cells (A, E), the total number of CD8<sup>+</sup> T cells (B, F), intratumoral PD-1<sup>+</sup>CD8<sup>+</sup> T cells (C, G) and total PD-1<sup>+</sup>CD8<sup>+</sup> T cells (D, H). The curve is the local regression curve (LOESS) between the two markers and  $\rho$  is the Spearman correlation coefficient. Infiltrating immune cells and the number of PD-L1<sup>+</sup> stromal/immune cells are represented on a  $\log_{10}$  scale.

PD-L1 expression by stromal cells of *ALK*-positive ADC was not associated with infiltration of PD-1<sup>+</sup>CD8<sup>+</sup> T cells or CD8<sup>+</sup> T cells (Figs. 6 E–H). Total CD4<sup>+</sup> T cell or regulatory T cell counts were not correlated with PD-L1 expression on tumor or stromal/immune cells (data not shown) and no correlation was observed between HLA-class I expression and PD-L1 expression by tumor or stromal cells or immune cell infiltration (data not shown).

### **ALK-positive ADC display various criteria associated with clinical response to PD-1-PD-L1 blockade**

Various authors have proposed to classify tumors based on their PD-L1 expression and tumor infiltration by CD8<sup>+</sup> T cells to more reliably predict tumors most likely to respond to blockade of the PD-1/PD-L1 pathway<sup>24,25</sup>. We defined composite predictive biomarkers combining PD-L1 expression by tumor cells (as defined by more than 10% of tumor cells expressing PD-L1) and mean intratumoral CD8<sup>+</sup> T cell or intratumoral PD-1<sup>+</sup>CD8<sup>+</sup> T cell counts higher than their respective medians (Figs. 7A and B). The percentage of patients displaying the two criteria of clinical response (% PD-L1 on tumor cells and infiltration by intratumoral PD-1<sup>+</sup>CD8<sup>+</sup> T cells or CD8<sup>+</sup> T cells) was higher in *ALK*-positive ADC than in *EGFR*-mutated and WT tumors (Figs. 7A and B). Indeed, 10 out of 29 patients (34%) in the *ALK*-positive group exhibited positive PD-L1 expression by tumor cells (cut-off 10%) with infiltration by PD-1<sup>+</sup>CD8<sup>+</sup> T cells higher than the median (Fig. 7B). In contrast, only 7% (2 out of 27) of *EGFR*-mutated tumors ( $p = 0.02$ ) and 8% of WT tumors ( $p = 0.024$ ) presented these two criteria. When these positive criteria for response to immunotherapy were combined with expression of MHC class I

molecules or PD-L1 expression by stromal/immune cells dichotomized by the median, no overall difference was observed between the various subgroups (Figs. 7C and D). However, the combination of PD-L1 expression on tumor cells and stromal cells and intratumoral infiltration by PD-1<sup>+</sup>CD8<sup>+</sup> T cells tended to be more frequent in *ALK*-positive ADC than in non-*ALK*-rearranged tumors (6/29 vs. 3/52,  $p = 0.063$ ) (Fig. 7D). In addition, PD-L1 expression and high HLA-class I expression on tumor cells with intratumoral infiltration by PD-1<sup>+</sup>CD8<sup>+</sup> T cells appeared to be more frequent in *ALK*-positive ADC (6/28: 21%, missing data for HLA class I expression in one case) compared with non-*ALK*-rearranged tumors (3/52: 6%) ( $p = 0.059$ ) (Fig. 7C).

In view of the heterogeneous PD-L1 expression and infiltration by CD8<sup>+</sup> T cells in *ALK*-positive ADC, we investigated whether tobacco might constitute a confounding factor in this analysis. No correlation was demonstrated between smoking status and PD-L1 expression by tumor cells or infiltration by PD-1<sup>+</sup>CD8<sup>+</sup> T cells in *ALK*-positive ADC (Table S3).

### **Relationship between tumor phenotype or immune cell infiltration and tumor aggressiveness and clinical outcome**

We next addressed whether the PD-L1 expression or immune cell infiltration was associated with tumor aggressiveness and clinical outcome. Neither PD-L1 expression by tumor cells nor total or intratumoral infiltration of PD-1<sup>+</sup>CD8<sup>+</sup> T cells were correlated with T, N or M staging, or tumor stage (Table S3). In line with these results, a more detailed analysis of the relationships between PD-L1 expression by tumor cells and/or stromal-immune cells and clinical outcome did not reveal any association with DFS or OS (Table S4). Similarly, no

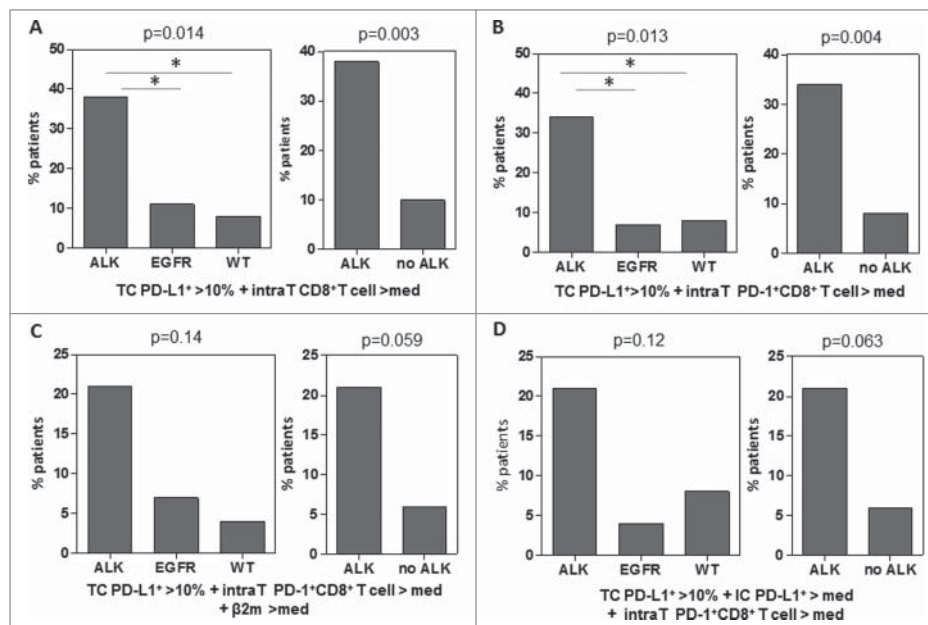


**Figure 7.** Composite predictive biomarkers are enriched in the *ALK*-positive lung cancer group. Various composite predictive biomarkers profiles of clinical response to blockade of the PD-1-PD-L1 pathway were defined based on criteria from the literature. Four composite biomarkers were presented. (A) PDL-1<sup>+</sup> on tumor cells > 10% and intratumoral (intraT) CD8<sup>+</sup> T cells > median (med). (B) PDL-1<sup>+</sup> on tumor cells > 10% and intratumoral PD-1<sup>+</sup>CD8<sup>+</sup> T cells > median. (C) PDL-1<sup>+</sup> on tumor cells > 10% and intratumoral PD-1<sup>+</sup>CD8<sup>+</sup> T cells > median and  $\beta 2$ -microglobulin > median. (D) PD-L1<sup>+</sup> on tumor cells > 10% and PD-L1<sup>+</sup> stromal/immune cells (IC) > median and intratumoral PD-1<sup>+</sup>CD8<sup>+</sup> T cells > median. The percentage of each subgroup of lung cancer patients (ALK-positive, EGFR- mutated, non-EGFR-mutated and non-KRAS-mutated and non-ALK-positive tumors) or after dichotomization between ALK-positive and non-ALK-positive tumors displaying these composite predictive biomarker is shown. The proportion of patients with composite biomarkers were compared between subgroups using Fisher's exact test.



relationship was observed between immune cell infiltration by CD8<sup>+</sup> T cells or PD-1<sup>+</sup> T cells or CD4<sup>+</sup> T cells or Foxp3<sup>+</sup>CD4<sup>+</sup> T cells and DFS or OS (Table S4). Composite biomarkers including PD-L1 expression by tumor cells and the levels of infiltration by intratumoral CD8<sup>+</sup> T cells or PD-1<sup>+</sup>CD8<sup>+</sup> T cells were not associated with clinical outcomes (Fig. S5). These biomarkers may therefore constitute predictive markers rather than prognostic markers in patients with *ALK*-positive ADC.

## Discussion

When tumors are classified according to their PD-L1 expression and tumor infiltration by CD8<sup>+</sup> T cells, it has been shown that the tumors most responsive to PD-1/PD-L1 blockade (melanoma, lung carcinoma, renal carcinoma) exhibit the highest frequencies of PD-L1-positive tumors combined with a high density of intratumoral CD8<sup>+</sup> T cell infiltration.<sup>24,25</sup> The present study demonstrated a higher frequency of tumors combining positive PD-L1 expression on tumor cells and infiltration by intratumoral CD8<sup>+</sup> T cells or PD-1<sup>+</sup>CD8<sup>+</sup> T cells in *ALK*-positive lung cancer patients than in *EGFR*-mutated ( $p = 0.03$ ) or non-*EGFR*-mutated and non-*K-RAS*-mutated lung cancer patients ( $p = 0.012$ ). As, in some studies, PD-L1 expression on both tumor cells and stromal cells contributed to clinical response.<sup>12,17</sup> We also showed that *ALK*-positive ADC preferentially belonged to the group with positive PD-L1 expression on tumor cells and stromal cells associated with intratumoral infiltration by PD-1<sup>+</sup>CD8<sup>+</sup> T cells, compared with non-*ALK*-rearranged lung cancer ( $p = 0.063$ ). Our results have not yet been validated by determination of clinical response in the subgroup of *ALK*-positive patients in a large series of lung cancer patients treated by immunotherapy. In a limited series of six *ALK*-positive ADC, no clinical response was obtained after administration of PD-1 inhibitors.<sup>31</sup> However, immunotherapy was mostly administered following disease progression on crizotinib. Interestingly, paired biopsies before and after crizotinib showed that crizotinib led to a decrease in PD-L1 expression and CD8<sup>+</sup> T cell infiltration.<sup>31</sup> In addition, *in vitro*, PD-L1 expression on tumor cells was downmodulated after treatment with specific *ALK* inhibitors or *ALK* siRNAs.<sup>29</sup> These data suggest that, on the basis of these predictive biomarkers (PD-L1, CD8<sup>+</sup> T cells), immunotherapy should be administered before crizotinib.

When immunohistochemical parameters composing the predictive signature were analyzed separately in more detail, to more precisely define the tumor microenvironment of *ALK*-positive ADC, we found a greater number of patients with positive PD-L1 expression on tumor cells in the *ALK*-positive group than in non-*ALK*-rearranged lung cancer patients. Various studies have also shown that PD-L1 expression, as detected by immunohistochemical analysis, was higher in NSCLC tumor specimens positive for *ALK* rearrangement than in control lung cancer.<sup>29,32,33</sup> In both anaplastic large cell lymphoma and *ALK*-positive lung cancer, the respective NPM-*ALK* and EML4-*ALK* chimeric proteins were shown to induce PD-L1 via distinct signaling mechanisms.<sup>28,29</sup> Interestingly, we found a very strong correlation between PD-L1 expression on tumor cells and intratumoral infiltration by CD8<sup>+</sup> T cells. In melanoma

patients, it has been demonstrated that the CD8<sup>+</sup> T cells in contact with the tumor produced IFN $\gamma$ , which upregulated PD-L1 expression.<sup>34</sup> A similar mechanism could also occur in *ALK*-positive lung cancer.

This relationship between PD-L1 expression on tumor cells and CD8<sup>+</sup> T cell infiltration was not observed in *EGFR*-mutated tumors and non-*EGFR*-mutated, non-*K-RAS*-mutated lung cancers, which reinforces the specificity of *ALK*-positive tumors for this additional mechanism of PD-L1 regulation. In *ALK*-positive lung cancer patients, the mechanisms of PD-L1 expression would result from both oncogenic events via the presence of the *ALK* chimeric protein and an adaptive mechanism based on the presence of infiltrating CD8<sup>+</sup> T cells.

No correlation was observed between PD-L1 expression on tumor cells and stromal/immune cells. In line with these results, no correlation was observed between PD-L1 expression on stromal/immune cells and CD8<sup>+</sup> T cell infiltration. Fehrenbacher et al. also reported distinct populations of lung cancer based on their PD-L1 expression on tumor cells or stromal cells.<sup>17</sup> IL-10 and IL-32B have been reported to induce PD-L1 on monocytes, but not on tumor cells, suggesting different mechanisms of regulation of PD-L1 in stroma and in the tumor nest.<sup>35</sup> However, in other studies, CD8<sup>+</sup> T cell infiltration was correlated with PD-L1 expression on immune cells in the stroma.<sup>12,17</sup>

Most studies have emphasized the role of pre-existing anti-tumor CD8<sup>+</sup> T cells in the efficacy of PD-1-PD-L1 blockade. Previous studies have reported that peptides derived from chimeric *ALK* protein could generate anti-*ALK*-specific CD8<sup>+</sup> T cells.<sup>36</sup> These cells have also been detected in cancer patients with *ALK* rearrangements.<sup>26,27</sup> We did not investigate the presence of anti-*ALK*-specific T cells in our series of *ALK*-positive ADC, but indirect arguments suggest that antitumor CD8<sup>+</sup> T cells were present. Most infiltrating CD8<sup>+</sup> T cells expressed PD-1 and specific T cells are known to be enriched in this PD-1-positive T cell population.<sup>37,38</sup> Close contact between PD-1<sup>+</sup>CD8<sup>+</sup> T cells and tumor cells was visualized *in situ*.

Based on our predictive criteria of response to immunotherapy, the group of *EGFR*-mutated cancer patients, who rarely co-expressed PD-L1 and rarely presented intratumoral infiltration by PD-1<sup>+</sup>CD8<sup>+</sup> T cells, could be considered to be less likely to respond to PD-1-PD-L1 blockade. This hypothesis has now been validated in various clinical trials.<sup>18,31,39</sup>

Several limitations of our study need to be mentioned. This analysis focused on predictive criteria of response to PD-1-PD-L1 blockade based on *in situ* multiparametric immunofluorescence analysis. Other biomarkers of clinical response measured by immunocytochemistry (PD-L2)<sup>17</sup> or gene expression analysis (IFN $\gamma$  or stromal signature)<sup>17,21,22,40</sup> or tumor sequencing (mutation load)<sup>10</sup> have also been reported and could have led to different conclusions. However, the relevance of these markers remains more controversial.<sup>21,23,41</sup> In addition, correlations have been previously reported between the biomarkers tested in our study and other potential predictive parameters, which mitigate this bias. Indeed, a positive association was found between patients belonging to the group with PD-L1-expressing tumors and CD8<sup>+</sup> T cell infiltration and those harboring high mutational load and *in silico* predicted mutant neoantigens.<sup>25</sup> Other studies have also demonstrated relationships

between total mutation load or mutated epitopes in the tumor and PD-L1 expression or cytolytic activity and CTL infiltration.<sup>42-44</sup>

One of our control groups (non-*EGFR*-mutated non-*K-RAS*-mutated lung cancer) could be heterogeneous and may have included patients with other mutations (*P53*, *Ros*, *STK11*, *Braf*, etc.), which could influence PD-L1 expression and the composition of the tumor microenvironment.<sup>45,46</sup> However, our other control group of *EGFR*-mutated lung tumors was well defined and homogeneous and *ALK*-positive lung cancer patients clearly displayed a higher frequency of predictive biomarkers of clinical response than this control group.

An immunogram based on various parameters that could influence cancer-immune interaction has recently been proposed.<sup>47</sup> The multiparametric *in situ* immunofluorescence technique developed in the present study is adapted to composite biomarkers requiring simultaneous measurement of predictive biomarkers of response to immunotherapy. Automated counting allows reproducible operator-independent results. This technique accurately enumerates cells with specific phenotypes and not simply surface area of staining, as a surrogate marker of infiltrating cells.<sup>31,48</sup> It allows precise localization of immune cells and PD-L1 in the tumor nests or in the stroma, which may modify the significance of these markers in terms of predictive and prognostic value.<sup>22</sup> In the literature, tumor cells are considered to express PD-L1 when staining is observed in the tumor nests. We clearly demonstrated PD-L1 expression by non-tumor cells in the tumor zone (Fig. 5) and only this type of multiparametric technique can avoid this bias.

Overall, based on this technique, this study suggests that a subgroup of *ALK*-positive lung cancer patients may constitute good candidates for anti-PD-1-PD-L1 therapy, but ideally before modification of the tumor microenvironment by crizotinib.

## Methods and patients

### Patient cohorts

A retrospective cohort of 29 patients with non-treated lung ADC with *ALK* rearrangement (*ALK*-positive) who underwent lobectomy in the thoracic surgery departments of five French Hospitals (Georges Pompidou, Tenon and Bichat, Paris; Louis Pasteur, Nice; Hautepierre, Strasbourg) was set up. Frozen sections of tumors before TKI therapy were available for each patient. As control groups, we selected *EGFR*-mutated tumors ( $n = 27$ ) and a population of lung cancers with no *EGFR* and no *K-RAS* mutations and without *ALK* rearrangement, hereafter defined as wild-type (WT) ( $n = 25$ ). *ALK* rearrangement was detected by break-apart fluorescent *in situ* hybridization. For the control groups, targeted next generation sequencing (NGS) using the Colon and LungV2 ampliseq panel (lifetechnologies) on a Ionproton sequencer was performed to determine the patient's molecular status (*EGFR* mutations, *K-RAS* mutations).

Characteristics of the *ALK*-positive patients are reported in Table S1. Pathological staging was reported according to the TNM 2009 classification. The median disease-free survival (DFS) and OS at the time of analysis were 37 mo and 72 mo,

respectively. Fifteen patients had been treated by chemotherapy and three patients received radiotherapy. The characteristics of *EGFR*-mutated tumors and WT tumors are also indicated in Table S1. As expected, male gender and smokers were more frequent in the WT group (Table S1). This study was conducted in accordance with the Declaration of Helsinki and was approved by the local ethics committee (CPP Ile de France II No. 2015-08-07). Informed consent was obtained from all participants.

### *In situ* immunofluorescence staining

Tissue samples obtained on the day of surgery were frozen and stored at  $-80^{\circ}\text{C}$ . Frozen specimens provided by the Biological Resources Center and Tumor Bank Platform were sectioned at 4 to 6  $\mu\text{m}$  with a cryostat, placed on slides, air-dried and fixed for 5 min with 100% acetone. Slides were pretreated with avidin/biotin blocker (Dako, Carpinteria, CA) for 10 min and Fc receptors were blocked with AB serum in PBS for 30 min.

The fields were selected by the presence of carcinomatous nests and validated by a pathologist. Slides and fields without tumor were excluded. PD-L1 expression on tumor cells was defined as a quantitative and qualitative variable. Only membranous staining of the tumor was considered and various cut-offs of 1%, 10%, 50% were examined for PD-L1 expression on tumor cells. When integrated in a composite biomarker, the cut-off of 10% was selected, as proposed in a recent meta-analysis, as the difference in clinical response between PD-L1 positive and negative patients was significantly higher in studies with a cut-off  $> 10\%$ .<sup>49</sup> PD-L1 expression on immune cells, PD-1<sup>+</sup>CD8<sup>+</sup> T cells, total CD8<sup>+</sup> T cells, total CD4<sup>+</sup> T cells, FoxP3<sup>+</sup>CD4<sup>+</sup> regulatory T cells were measured as quantitative variables (mean number of cells per field). Three multiplex stainings were performed using labeled or unlabeled primary antibodies followed by fluorophore-labeled secondary antibodies: quadruplex staining for PD-L1, PD-1, cytokeratin 19 and CD8<sup>+</sup>, triplex staining for CD4<sup>+</sup>, Foxp3 and cytokeratin 19 (CK19) and double staining for pankeratin AE1/AE3 and  $\beta$ 2-microglobulin. These antibodies are detailed in Table S2. Isotype-matched antibodies were used as negative controls. In each case, we checked that the secondary antibodies did not cross-react with unrelated primary antibodies used in the combination. Nuclei were highlighted using DAPI mounting medium.

### Fluorescence analysis and automated cell count

Slides of stained lung sections were read with a Vectra<sup>®</sup> automated microscope. This Perkin Elmer<sup>®</sup> technology allows measurement of morphometric and fluorescence characteristics in the various cell compartments (membrane/cytoplasm/nuclei). An associated cell analysis software, inForm<sup>®</sup>, integrates these various signals, allowing a multiplex staining protocol. As recommended for multiplex analysis, single-stained (Cyanine 2 or Cyanine 3 or Alexa Fluor 594 or APC) and non-stained slides were analyzed with inForm<sup>®</sup> to integrate the corresponding spectra into a fluorescence library.

For each slide, image acquisition and subsequent cell counts were performed on at least five fields using a 20  $\times$  objective, except for  $\beta$ 2-microglobulin staining, which was done on at



least two fields. For each patient, results correspond to the mean of various fields. Briefly, “tissue segmentation” was performed on the basis of cytokeratin staining (CK19 or AE1-AE3), and “cell segmentation” was performed on the basis of DAPI staining and the size of the cells. Tissue and cell recognition, integrated by InForm<sup>®</sup> software allowed to define the localization of each marker in the tumor nest (intratumoral) or stroma (peritumoral). A phenotyping step based on “training” of the software to recognize positive and negative cells, resulting in an analysis algorithm, was then performed. Mapping determined the phenotype of the cells with each color point corresponding to the number of single-stained, double-stained or triple-stained cells (see figure legends). A semiquantitative *H score* established by InForm<sup>®</sup> software based on the percentage of tumor cells expressing  $\beta 2$ -microglobulin (0–100%) and the staining intensity ranging from 1 to 3 was then used to determine  $\beta 2$ -microglobulin expression by tumor cells. The H-score corresponds to the product of these two results (the maximum value of 300 corresponded to 100% of  $\beta 2$ -microglobulin-positive tumor cells with an intensity score of 3). Each phenotyping image was checked by a pathologist after software analysis.

### Statistical analysis

Continuous variables are expressed as the median and interquartile range and were compared between groups using Wilcoxon’s rank sum test or Kruskal–Wallis test when appropriate. Categorical variables are expressed as numbers and percentages and were compared using Fisher’s exact test. Correlation between biomarker expression was estimated with Spearman’s rank correlation coefficient. OS of *ALK*-positive patients was defined as the time from the date of surgery to the date of death or last follow-up. Disease-free survival (DFS) was defined as the time from the date of surgery to the date of recurrence diagnosis, death or last follow-up, whichever occurred first. OS and DFS were estimated using the Kaplan–Meier method. Association between clinical variables and biomarkers with OS and DFS were estimated in Cox models. Proportional hazards hypothesis and log linearity of continuous variables were assessed. All tests were two-sided and *p*-values less than 0.05 indicated significant associations. Analyses were performed on R statistical platform, version 3.1.1.

### Disclosure of potential conflicts of interest

No potential conflicts of interest were disclosed.

### Acknowledgments

We would like to thank Dr Bebieuvre, E. Bergman and E. Selva for their support as well as the staff of the Biological Resources Center and Tumor Bank Platform of Hôpital European Georges Pompidou (BB-0033–00063), Hôpital Tenon, Hôpital de Hautepierre in Strasbourg and Hôpital Louis Pasteur in Nice for providing sample materials and the Histology platform of PARCC European Georges Pompidou.

### Funding

This work was supported by grants from Pfizer (JC, ET), Ligue contre le Cancer (ET), Université Sorbonne Paris Cité (ET), ANR (Selectimmunco)

(ET), Labex Immuno-Oncology (ET), SIRIC CARPEM (ET), and Fondation ARC (EG).

### References

- Boi M, Zucca E, Inghirami G, Bertoni F. Advances in understanding the pathogenesis of systemic anaplastic large cell lymphomas. *Br J Haematol* 2015; 168(6):771–83; PMID:25559471; <http://dx.doi.org/10.1111/bjh.13265>
- Shaw AT, Hsu PP, Awad MM, Engelman JA. Tyrosine kinase gene rearrangements in epithelial malignancies. *Nat Rev Cancer* 2013; 13(11):772–87; PMID:24132104; <http://dx.doi.org/10.1038/nrc3612>
- Soda M, Choi YL, Enomoto M, Takada S, Yamashita Y, Ishikawa S, Fujiwara S, Watanabe H, Kurashina K, Hatanaka H et al. Identification of the transforming EML4-ALK fusion gene in non-small-cell lung cancer. *Nature* 2007; 448(7153):561–6; PMID:17625570; <http://dx.doi.org/10.1038/nature05945>
- Barlesi F, Mazieres J, Merlio JP, Debieuvre D, Mosser J, Lena H, Ouafik L, Besse B, Rouquette I, Westeel V et al. Routine molecular profiling of patients with advanced non-small-cell lung cancer: Results of a 1-year nationwide programme of the French Cooperative Thoracic Intergroup (IFCT). *Lancet* 2016; 387(10026):1415–26; PMID:26777916; [http://dx.doi.org/10.1016/S0140-6736\(16\)00004-0](http://dx.doi.org/10.1016/S0140-6736(16)00004-0)
- Camidge DR, Pao W, Sequist LV. Acquired resistance to TKIs in solid tumours: Learning from lung cancer. *Nat Rev Clin Oncol* 2014; 11(8):473–81; PMID:24981256; <http://dx.doi.org/10.1038/nrclinonc.2014.104>
- Brahmer J, Reckamp KL, Baas P, Crino L, Eberhardt WE, Poddubskaya E, Antonia S, Pluzanski A, Vokes EE, Holgado E et al. Nivolumab versus docetaxel in advanced squamous-cell non-small-cell lung cancer. *N Engl J Med* 2015; 373(2):123–35; PMID:26028407; <http://dx.doi.org/10.1056/NEJMoa1504627>
- Borghaei H, Paz-Ares L, Horn L, Spigel DR, Steins M, Ready NE, Chow LQ, Vokes EE, Felip E, Holgado E et al. Nivolumab versus docetaxel in advanced nonsquamous non-small-cell lung cancer. *N Engl J Med* 2015; 373(17):1627–39; PMID:26412456; <http://dx.doi.org/10.1056/NEJMoa1507643>
- Herbst RS, Baas P, Kim DW, Felip E, Perez-Gracia JL, Han JY, Molina J, Kim JH, Arvis CD, Ahn MJ et al. Pembrolizumab versus docetaxel for previously treated, PD-L1-positive, advanced non-small-cell lung cancer (KEYNOTE-010): A randomised controlled trial. *Lancet* 2016; 387(10027):1540–50; PMID:26712084; [http://dx.doi.org/10.1016/S0140-6736\(15\)01281-7](http://dx.doi.org/10.1016/S0140-6736(15)01281-7)
- Yadav M, Delamarre L. Immunotherapy. Outsourcing the immune response to cancer. *Science* 2016; 352(6291):1275–6; PMID:27284181; <http://dx.doi.org/10.1126/science.aag1547>
- Rizvi NA, Hellmann MD, Snyder A, Kvistborg P, Makarov V, Havel JJ, Lee W, Yuan J, Wong P, Ho TS et al. Cancer immunology. Mutational landscape determines sensitivity to PD-1 blockade in non-small cell lung cancer. *Science* 2015; 348(6230):124–8; PMID:25765070; <http://dx.doi.org/10.1126/science.aaa1348>
- Le DT, Uram JN, Wang H, Bartlett BR, Kemberling H, Eyring AD, Skora AD, Lubner BS, Azad NS, Laheru D et al. PD-1 blockade in tumors with mismatch-repair deficiency. *N Engl J Med* 2015; 372(26):2509–20; PMID:26028255; <http://dx.doi.org/10.1056/NEJMoa1500596>
- Rosenberg JE, Hoffman-Censits J, Powles T, van der Heijden MS, Balar AV, Necchi A, Dawson N, O’Donnell PH, Balmanoukian A, Loriot Y et al. Atezolizumab in patients with locally advanced and metastatic urothelial carcinoma who have progressed following treatment with platinum-based chemotherapy: A single-arm, multicentre, phase 2 trial. *Lancet* 2016; 387(10031):1909–20; PMID:26952546; [http://dx.doi.org/10.1016/S0140-6736\(16\)00561-4](http://dx.doi.org/10.1016/S0140-6736(16)00561-4)
- Bouffet E, Larouche V, Campbell BB, Merico D, de Borja R, Aronson M, Durno C, Krueger J, Cabric V, Ramaswamy V et al. Immune checkpoint inhibition for hypermutant glioblastoma multiforme resulting from germline biallelic mismatch repair deficiency. *J Clin Oncol* 2016; 34(19):2206–11; PMID:27001570; <http://dx.doi.org/10.1200/JCO.2016.66.6552>

14. Motzer RJ, Escudier B, McDermott DF, George S, Hammers HJ, Srinivas S, Tykodi SS, Sosman JA, Procopio G, Plimack ER et al. Nivolumab versus everolimus in advanced renal-cell carcinoma. *N Engl J Med* 2015; 373(19):1803-13; PMID:26406148; <http://dx.doi.org/10.1056/NEJMoa1510665>
15. Tran E, Ahmadzadeh M, Lu YC, Gros A, Turcotte S, Robbins PF, Gartner JJ, Zheng Z, Li YF, Ray S et al. Immunogenicity of somatic mutations in human gastrointestinal cancers. *Science* 2015; 350(6266):1387-90; PMID:26516200; <http://dx.doi.org/10.1126/science.aad1253>
16. Garon EB, Rizvi NA, Hui R, Leigh N, Balmanoukian AS, Eder JP, Patnaik A, Aggarwal C, Gubens M, Horn L et al. Pembrolizumab for the treatment of non-small-cell lung cancer. *N Engl J Med* 2015; 372(21):2018-28; PMID:25891174; <http://dx.doi.org/10.1056/NEJMoa1501824>
17. Fehrenbacher L, Spira A, Ballinger M, Kowanetz M, Vansteenkiste J, Mazieres J, Park K, Smith D, Artal-Cortes A, Lewanski C et al. Atezolizumab versus docetaxel for patients with previously treated non-small-cell lung cancer (POPLAR): A multicentre, open-label, phase 2 randomised controlled trial. *Lancet* 2016; 387(10030):1837-46; PMID:26970723; [http://dx.doi.org/10.1016/S0140-6736\(16\)00587-0](http://dx.doi.org/10.1016/S0140-6736(16)00587-0)
18. Gettinger S, Rizvi NA, Chow LQ, Borghaei H, Brahmer J, Ready N, Gerber DE, Shepherd FA, Antonia S, Goldman JW et al. Nivolumab monotherapy for first-line treatment of advanced non-small-cell lung cancer. *J Clin Oncol* 2016; 34(25):2980-7; PMID:27354485; <http://dx.doi.org/10.1200/JCO.2016.66.9929>
19. Tumeh PC, Harview CL, Yearley JH, Shintaku IP, Taylor EJ, Robert L, Chmielowski B, Spasic M, Henry G, Ciobanu V et al. PD-1 blockade induces responses by inhibiting adaptive immune resistance. *Nature* 2014; 515(7528):568-71; PMID:25428505; <http://dx.doi.org/10.1038/nature13954>
20. Taube JM, Klein A, Brahmer JR, Xu H, Pan X, Kim JH, Chen L, Pardoll DM, Topalian SL, Anders RA. Association of PD-1, PD-1 ligands, and other features of the tumor immune microenvironment with response to anti-PD-1 therapy. *Clin Cancer Res* 2014; 20(19):5064-74; PMID:24714771; <http://dx.doi.org/10.1158/1078-0432.CCR-13-3271>
21. Hugo W, Zaretsky JM, Sun L, Song C, Moreno BH, Hu-Lieskovan S, Berent-Maoz B, Pang J, Chmielowski B, Cherry G et al. Genomic and transcriptomic features of response to anti-pd-1 therapy in metastatic melanoma. *Cell* 2016; 165(1):35-44; PMID:26997480; <http://dx.doi.org/10.1016/j.cell.2016.02.065>
22. Herbst RS, Soria JC, Kowanetz M, Fine GD, Hamid O, Gordon MS, Sosman JA, McDermott DF, Powderly JD, Gettinger SN et al. Predictive correlates of response to the anti-PD-L1 antibody MPDL3280A in cancer patients. *Nature* 2014; 515(7528):563-7; PMID:25428504; <http://dx.doi.org/10.1038/nature14011>
23. McDermott DF, Sosman JA, Sznol M, Massard C, Gordon MS, Hamid O, Powderly JD, Infante JR, Fasso M, Wang YV et al. Atezolizumab, an anti-programmed death-ligand 1 antibody, in metastatic renal cell carcinoma: Long-term safety, clinical activity, and immune correlates from a phase Ia study. *J Clin Oncol* 2016; 34(8):833-42; PMID:26755520; <http://dx.doi.org/10.1200/JCO.2015.63.7421>
24. Teng MW, Ngiow SF, Ribas A, Smyth MJ. Classifying cancers based on T-cell infiltration and PD-L1. *Cancer Res* 2015; 75(11):2139-45; PMID:25977340; <http://dx.doi.org/10.1158/0008-5472.CAN-15-0255>
25. Ock CY, Keam B, Kim S, Lee JS, Kim M, Kim TM, Jeon YK, Kim DW, Chung DH, Heo DS. Pan-cancer immunogenomic perspective on the tumor microenvironment based on PD-L1 and CD8 T-cell infiltration. *Clin Cancer Res* 2016; 22(9):2261-70; PMID:26819449; <http://dx.doi.org/10.1158/1078-0432.CCR-15-2834>
26. Ait-Tahar K, Cerundolo V, Banham AH, Hatton C, Blanchard T, Kusec R, Becker M, Smith GL, Pulford K. B and CTL responses to the ALK protein in patients with ALK-positive ALCL. *Int J Cancer* 2006; 118(3):688-95; PMID:16114011; <http://dx.doi.org/10.1002/ijc.21410>
27. Passoni L, Gallo B, Biganzoli E, Stefanoni R, Massimino M, Di Nicola M, Gianni AM, Gambacorti-Passerini C. In vivo T-cell immune response against anaplastic lymphoma kinase in patients with anaplastic large cell lymphomas. *Haematologica* 2006; 91(1):48-55; PMID:16434370
28. Marzec M, Zhang Q, Goradia A, Raghunath PN, Liu X, Paessler M, Wang HY, Wysocka M, Cheng M, Ruggeri BA et al. Oncogenic kinase NPM/ALK induces through STAT3 expression of immunosuppressive protein CD274 (PD-L1, B7-H1). *Proc Natl Acad Sci U S A* 2008; 105(52):20852-7; PMID:19088198; <http://dx.doi.org/10.1073/pnas.0810958105>
29. Ota K, Azuma K, Kawahara A, Hattori S, Iwama E, Tanizaki J, Harada T, Matsumoto K, Takayama K, Takamori S et al. Induction of PD-L1 expression by the EML4-ALK oncoprotein and downstream signaling pathways in non-small cell lung cancer. *Clin Cancer Res* 2015; 21(17):4014-21; PMID:26019170; <http://dx.doi.org/10.1158/1078-0432.CCR-15-0016>
30. Voena C, Menotti M, Mastini C, Di Giacomo F, Longo DL, Castella B, Merlo ME, Ambrogio C, Wang Q, Minero VG et al. Efficacy of a cancer vaccine against ALK-rearranged lung tumors. *Cancer Immunol Res* 2015; 3(12):1333-43; PMID:26419961; <http://dx.doi.org/10.1158/2326-6066.CIR-15-0089>
31. Gainor JF, Shaw AT, Sequist LV, Fu X, Azzoli CG, Piotrowska Z, Huynh TG, Zhao L, Fulton L, Schultz KR et al. EGFR mutations and ALK rearrangements are associated with low response rates to PD-1 pathway blockade in non-small cell lung cancer: A retrospective analysis. *Clin Cancer Res* 2016; 22(18):4585-93; PMID:27225694; <http://dx.doi.org/10.1158/1078-0432.CCR-15-3101>
32. Koh J, Go H, Keam B, Kim MY, Nam SJ, Kim TM, Lee SH, Min HS, Kim YT, Kim DW et al. Clinicopathologic analysis of programmed cell death-1 and programmed cell death-ligand 1 and 2 expressions in pulmonary adenocarcinoma: Comparison with histology and driver oncogenic alteration status. *Mod Pathol* 2015; 28(9):1154-66; PMID:26183759; <http://dx.doi.org/10.1038/modpathol.2015.63>
33. D'Incecco A, Andreozzi M, Ludovini V, Rossi E, Capodanno A, Landi L, Tibaldi C, Minuti G, Salvini J, Coppi E et al. PD-1 and PD-L1 expression in molecularly selected non-small-cell lung cancer patients. *Br J Cancer* 2015; 112(1):95-102; PMID:25349974; <http://dx.doi.org/10.1038/bjc.2014.555>
34. Taube JM, Anders RA, Young GD, Xu H, Sharma R, McMiller TL, Chen S, Klein AP, Pardoll DM, Topalian SL et al. Colocalization of inflammatory response with b7-h1 expression in human melanocytic lesions supports an adaptive resistance mechanism of immune escape. *Sci Transl Med* 2012; 4(127):127ra37; PMID:22461641; <http://dx.doi.org/10.1126/scitranslmed.3003689>
35. Taube JM, Young GD, McMiller TL, Chen S, Salas JT, Pritchard TS, Xu H, Meeker AK, Fan J, Cheadle C et al. Differential expression of immune-regulatory genes associated with PD-L1 display in melanoma: Implications for PD-1 pathway blockade. *Clin Cancer Res* 2015; 21(17):3969-76; PMID:25944800; <http://dx.doi.org/10.1158/1078-0432.CCR-15-0244>
36. Yoshimura M, Tada Y, Ofuzi K, Yamamoto M, Nakatsura T. Identification of a novel HLA-A 02:01-restricted cytotoxic T lymphocyte epitope derived from the EML4-ALK fusion gene. *Oncol Rep* 2014; 32(1):33-9; PMID:24842630
37. Badoual C, Hans S, Merillon N, Van Ryswick C, Ravel P, Benhamouda N, Levionnois E, Nizard M, Si-Mohamed A, Besnier N et al. PD-1-expressing tumor-infiltrating T cells are a favorable prognostic biomarker in HPV-associated head and neck cancer. *Cancer Res* 2013; 73(1):128-38; PMID:23135914; <http://dx.doi.org/10.1158/0008-5472.CAN-12-2606>
38. Gros A, Parkhurst MR, Tran E, Pasetto A, Robbins PF, Ilyas S, Prickett TD, Gartner JJ, Crystal JS, Roberts IM et al. Prospective identification of neoantigen-specific lymphocytes in the peripheral blood of melanoma patients. *Nat Med* 2016; 22(4):433-8; PMID:26901407; <http://dx.doi.org/10.1038/nm.4051>
39. Hellmann MD, Gettinger S, JW G, Brahmer J, Borghaei H, Chow LQ, Ready N, Gerber DE, Juergens R, Shepherd F et al. Check-Mate 012: Safety and efficacy of first-line (1L) nivolumab (nivo; N) and ipilimumab (ipi; I) in advanced (adv) NSCLC. *J Clin Oncol* 2016; 34.
40. Seiwert TY, Burtneess B, Mehra R, Weiss J, Berger R, Eder JP, Heath K, McClanahan T, Lunceford J, Gause C et al. Safety and clinical activity of pembrolizumab for treatment of recurrent or metastatic squamous cell carcinoma of the head and neck

- (KEYNOTE-012): an open-label, multicentre, phase 1b trial. *Lancet Oncol* 2016; 17(7):956-65; PMID:27247226; [http://dx.doi.org/10.1016/S1470-2045\(16\)30066-3](http://dx.doi.org/10.1016/S1470-2045(16)30066-3)
41. McGranahan N, Furness AJ, Rosenthal R, Ramskov S, Lyngaa R, Saini SK, Jamal-Hanjani M, Wilson GA, Birkbak NJ, Hiley CT et al. Clonal neoantigens elicit T cell immunoreactivity and sensitivity to immune checkpoint blockade. *Science* 2016; 351(6280):1463-9; PMID:26940869; <http://dx.doi.org/10.1126/science.aaf1490>
  42. Chen DS, Irving BA, Hodi FS. Molecular pathways: Next-generation immunotherapy—inhibiting programmed death-ligand 1 and programmed death-1. *Clin Cancer Res* 2012; 18(24):6580-7; PMID:23087408; <http://dx.doi.org/10.1158/1078-0432.CCR-12-1362>
  43. Rooney MS, Shukla SA, Wu CJ, Getz G, Hacohen N. Molecular and genetic properties of tumors associated with local immune cytolytic activity. *Cell* 2015; 160(1-2):48-61; PMID:25594174; <http://dx.doi.org/10.1016/j.cell.2014.12.033>
  44. Brown SD, Warren RL, Gibb EA, Martin SD, Spinelli JJ, Nelson BH, Holt RA. Neo-antigens predicted by tumor genome meta-analysis correlate with increased patient survival. *Genome Res* 2014; 24(5):743-50; PMID:24782321; <http://dx.doi.org/10.1101/gr.165985.113>
  45. Mansuet-Lupo A, Alifano M, Pecuchet N, Biton J, Becht E, Goc J, Germain C, Ouakrim H, Regnard JF, Cremer I et al. Intratumoral immune cell densities are associated with lung adenocarcinoma gene alterations. *Am J Respir Crit Care Med* 2016; 194(11):1403-1412; PMID:27299180
  46. Cha YJ, Kim HR, Lee CY, Cho BC, Shim HS. Clinicopathological and prognostic significance of programmed cell death ligand-1 expression in lung adenocarcinoma and its relationship with p53 status. *Lung Cancer* 2016; 97:73-80; PMID:27237031; <http://dx.doi.org/10.1016/j.lungcan.2016.05.001>
  47. Blank CU, Haanen JB, Ribas A, Schumacher TN. Cancer immunology. The “cancer immunogram.” *Science* 2016; 352(6286):658-60; PMID:27151852; <http://dx.doi.org/10.1126/science.aaf2834>
  48. Bougherara H, Mansuet-Lupo A, Alifano M, Ngo C, Damotte D, Le Frere-Belda MA, Donnadieu E, Peranzoni E. Real-time imaging of resident T cells in human lung and ovarian carcinomas reveals how different tumor microenvironments control T lymphocyte migration. *Front Immunol* 2015; 6:500; PMID:26528284; <http://dx.doi.org/10.3389/fimmu.2015.00500>
  49. Carbognin L, Pilotto S, Milella M, Vaccaro V, Brunelli M, Calio A, Cuppone F, Sperduti I, Giannarelli D, Chilosi M et al. Differential activity of nivolumab, pembrolizumab and MPDL3280A according to the tumor expression of programmed death-ligand-1 (PD-L1): Sensitivity analysis of trials in melanoma, lung and genitourinary cancers. *PLoS One* 2015; 10(6):e0130142; PMID:26086854; <http://dx.doi.org/10.1371/journal.pone.0130142>